JACS
JOURNAL OF THE AMERICAN CHEMICAL SOCIETY
Article
pubs.acs.org/JACS

Revisiting the Radical Initiation Mechanism of the Diamine-Promoted Transition-Metal-Free Cross-Coupling Reaction

Li Zhang, Huan Yang, and Lei Jiao*

Center of Basic Molecular Science (CBMS), Department of Chemistry, Tsinghua University, Beijing 100084, China

Supporting Information

ABSTRACT: Radical chain reactions leading to C−C bond formation are widely used in organic synthesis, and initiation of the radical chain process usually requires thermolabile radical initiators. Recent studies on transition-metal-free cross-coupling reactions between aryl halides and arenes have demonstrated an unprecedented initiation system for radical chain reactions, where the combination of simple organic additives and a base was used in place of conventional radical initiators. Among them, the combination of *N*,*N*′-dimethylethylenediamine (DMEDA) and *t*-BuOK is one of the most efficient and representative reaction systems, and the radical initiation mechanism of this system has attracted considerable research interest. In this study, through the combination of kinetic studies, deuterium labeling experiments, and DFT calculations, the radical initiation mechanism of the diamine-promoted cross-coupling reaction was carefully reinvestigated. In light of the present study, a mechanistic network of radical initiation in the DMEDA/*t*-BuOK system was revealed, which differs dramatically from the previously realized single radical initiation pathway. In this mechanism, the diamine acts as a hydrogen atom donor and plays a dual role as both "radical amplifier" and "radical regulator" to initiate the radical chain process as well as to control the concentration of reactive radical species. This represents a rare example of a structurally simple molecule playing such a subtle role in the radical chain reaction system. The present study sheds some light on the novel radical initiation mode in transition-metal-free cross-coupling reactions following a base-promoted homolytic aromatic substitution (BHAS) mechanism, and may also help to understand the mechanism of relevant reactions.

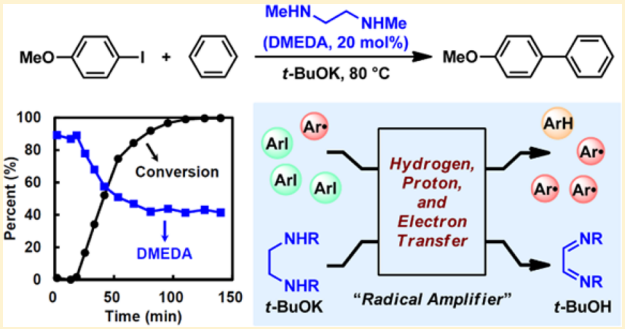

INTRODUCTION

Free-radical reactions constitute an important reaction category in organic chemistry.[1] Among them, C−C bond formation through radical chain process has contributed greatly to the toolbox for synthetic chemists.[2] Radical initiation is a significant process in radical chain reactions. For synthetic reactions involving a radical chain process, thermal decomposition of radical initiators is the most often used initiation method compared with others (e.g., photolysis and radiation).[1−3] Organic molecules with thermolabile chemical bonds that could undergo homolysis upon heating, such as peroxides (e.g., benzoyl peroxide, BPO) and azo compounds (e.g., 2,2′-azoisobutyronitrile, AIBN), are usually employed as radical initiators.

Since 2008,[4] studies on transition-metal-free C−C cross-coupling reactions[5] have shown that radical chain reactions could be initiated in a rather different way. Traditional cross-coupling reactions employ transition metal complexes as catalysts to promote the cross-coupling process through organometallic mechanism.[6] Recent studies have established a distinct approach, in which coupling between aryl halides and arenes (or olefins) is promoted by small molecule organic additives in the presence of base through radical chain mechanism (Scheme 1).[7−11] These transition-metal-free coupling reactions, classified as the base-promoted homolytic aromatic substitution (BHAS) reaction,[12] include inter/intramolecular coupling between aryl halides and arenes to form biaryls,[7−9] and Heck-type coupling between aryl halides and olefins to form aryl-substituted alkenes,[10] in which formal C−H arylations are achieved. A wide variety of organic additives, such as 1,10-phenanthrolines,[7b,c,m,s,w,8a,c,d,f,g,9e,10b,c] 1,2-diamines,[7a,s,8d,g] alcohols and 1,2-diols,[7l,o,u,8a,e,10a] amino acids,[7d,f] hydrazine derivatives,[7n,p] and *N*-heterocyclic carbenes,[7h] have been proved effective promotors for these reactions. Interestingly, although these organic additives (most of them are thermostable molecules) are distinct from conventional radical initiators, they initiate the radical chain process efficiently. The development of these reactions not only brought about new advances in cross-coupling methodology, but also enabled an unprecedented initiation system for radical chain reactions.

The radical initiation mechanism of these reaction systems has been a problem of interest in radical chemistry since their discovery. To date, the cross-coupling (chain propagation) mechanism has been made clear.[12] It is generally accepted that the generation of aryl radical from aryl halide and addition of the aryl radical to arene are key steps for cross-coupling, and

Received: April 4, 2016
Published: May 26, 2016

DOI: 10.1021/jacs.6b03442
J. Am. Chem. Soc. 2016, 138, 7151−7160

subsequent deprotonation, single electron transfer (SET), and C—X bond cleavage sustain the chain process (Scheme 1b).

Scheme 1. Transition-Metal-Free Cross-Coupling Reaction between Aryl Halides and Arenes (Ar = Aryl Group)

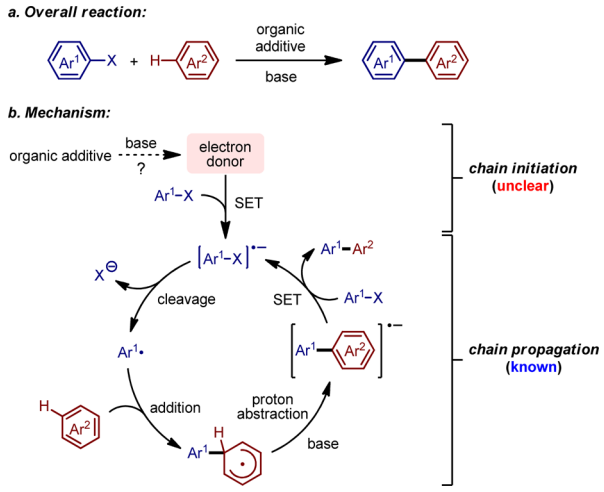

However, the chain initiation mechanism with various "unconventional initiators" still remains elusive, and only limited experimental efforts have been made to address this issue.[10d,12e,f,h] A general mechanistic interpretation is that the organic additive either directly functions as an electron donor or generates an electron donor under the reaction conditions, which then undergoes electron transfer to aryl halide to produce aryl radical as the initiator radical (Scheme 1b),[12] but the initiation mechanism has not been revealed in sufficient detail. To understand the nature of this novel radical initiation system and to utilize it in designing new radical chain reactions for synthesis, it is important to clearly identify the role of the organic additives through in-depth mechanistic studies.

Among the reaction systems that could initiate the transition-metal-free cross-coupling, the combination of *N*,*N*′-dimethylethylenediamine (DMEDA) and *t*-BuOK is a most effective and representative one.[7a,s,8d,g,13] As a consequence, the role of this structurally simple diamine in radical initiation attracted much research interest. Recently, Murphy, Tuttle, and co-workers reported their studies on the DMEDA/*t*-BuOK-promoted cross-coupling reactions,[12e] in which a redox-type radical initiation pathway was proposed. However, the results of the present study contradicted this mechanism, which prompted us to revisit the radical initiation process in this reaction system. Through detailed mechanistic study, a significantly different radical initiation mechanism has been revealed.

Herein, we present the details of our mechanistic study on the transition-metal-free coupling reaction utilizing the DMEDA/*t*-BuOK system. The study was conducted using a combined experimental and DFT computational approach, in which kinetic analysis and isotope labeling experiments played a crucial role. The present study revealed that an unconventional radical initiation mechanistic network, rather than a single initiation pathway, functioned in the reaction system. The diamine was found to act as a hydrogen atom donor and played a dual role as both "radical amplifier" and "radical regulator" in the radical chain process, which is distinct from previously realized. The transition-metal-free coupling reactions promoted by structurally related molecules (such as aminoalcohols[7a,8d,g] and diols[7a,8e]) might also be understood considering this mechanism.

RESULTS AND DISCUSSION

The aim of this research is to elucidate the role of diamine in the radical initiation process. An extensive literature survey showed that, in transition-metal-free cross-coupling reactions, organic additives were generally believed to function as electron donors,[12c,d] ligands,[7b,c,f,h,j,k,m,o,q,8a,c,d,f,g] or precursors to electron donors.[7e,n,p,12e] In the DMEDA/*t*-BuOK reaction system, possible initiation mechanisms include: (a) direct single electron transfer from DMEDA to the aryl halide; (b) DMEDA acting as a ligand to form alkali metal alkoxide complex, which then transfers an electron to the aryl halide; (c) DMEDA being converted to an electron-rich intermediate under the reaction conditions, which then acts as an electron donor to initiate the reaction (Scheme 2).

Scheme 2. Possible Initiation Mechanisms of the DMEDA/*t*-BuOK Reaction System

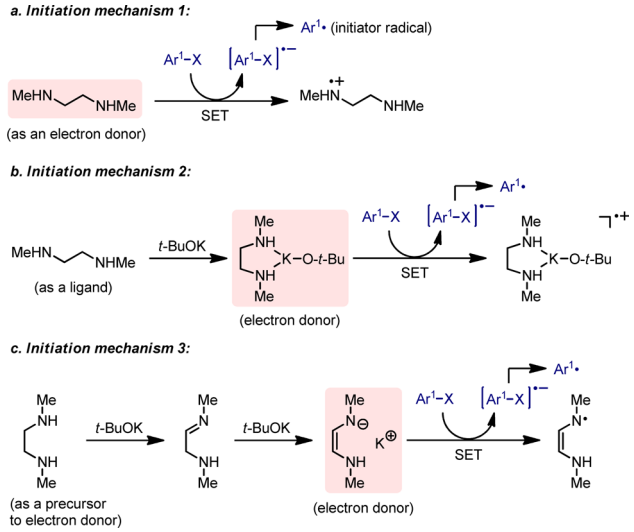

Murphy, Tuttle, and co-workers found that ethylene-deuterated DMEDA derivatives exhibited no radical initiation activity.[12e] On this basis, they concluded that cleavage of the C—H bond on the ethylene group played a critical role in the radical initiation process. Therefore, *initiation mechanisms 1 and 2* were believed to be unreasonable, and *initiation mechanism 3* was proposed: DMEDA is oxidized under basic conditions to generate an enamine-type electron donor, which then undergoes SET with aryl iodide to form an aryl radical as the initiator radical (Scheme 2). The involvement of methylene C—H bond cleavage in the oxidation step might account for the inactivity of methylene-deuterated DMEDA derivatives. However, no further details regarding the radical initiation mechanism were disclosed in their study. Our own study also excluded *initiation mechanisms 1 and 2*, because electrochemical measurements showed a large potential gap (ΔE = 3.5 V) between the oxidation of either DMEDA or the DMEDA/*t*-BuOK mixture and the reduction of aryl iodide (see the Supporting Information for details).

Reaction kinetics is a powerful tool for identification of possible reaction mechanisms and for exclusion of unreasonable ones.[14] To our surprise, to date kinetic analyses have not been conducted on these transition-metal-free cross-coupling reactions.[15] Aiming to disclose more details in the radical initiation mechanism of the DMEDA/*t*-BuOK reaction system, we monitored the kinetic profile of a model cross-coupling reaction, which unexpectedly revealed the contradiction between experimental results and this initiation mechanism.

DOI: 10.1021/jacs.6b03442
J. Am. Chem. Soc. 2016, 138, 7151−7160

Kinetic Profiles of the DMEDA-Promoted Cross-Coupling Reaction. The coupling reaction between 4-iodoanisole (**1**) and benzene was selected as a suitable model reaction for kinetic study, which affords a good yield of 4-methoxybiphenyl (**2**) in the presence of a catalytic amount of DMEDA and excess *t*-BuOK at 80 °C. Our study commenced with acquiring kinetic profiles of all components in the model reaction. The kinetic measurement was performed under the synthetically relevant conditions, except that a large excess of *t*-BuOK (≥10 equiv) was used to maintain its concentration constant during the reaction. It was found that the reaction exhibited a significant induction period (ca. 20 min), after which it completed in 2 h with 75% yield (Figure 1). Dehalogenation

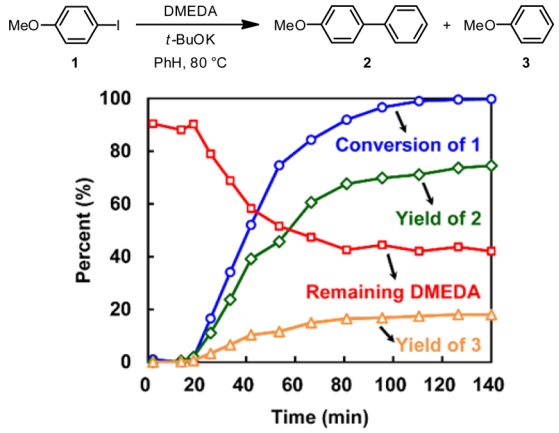

Figure 1. Kinetic profiles of aryl iodide **1** (blue), product **2** (green), byproduct **3** (orange), and DMEDA (red) in the model reaction. Reaction conditions: [DMEDA] = 22 mM, [**1**] = 108.5 mM, [*t*-BuOK] = 1.25 M, benzene as the solvent, 80 °C.

product anisole (**3**) was observed to generate simultaneously with product **2** as the major byproduct (18% yield). The kinetic profile of DMEDA was rather unexpected. DMEDA almost remained intact during the induction period, and was consumed when the coupling reaction started to proceed. After the reaction completed, the consumption of DMEDA also stopped (Figure 1). This indicated that the decay of DMEDA was highly dependent on the main chain reaction. This kinetic profile is unprecedented for conventional radical initiators; it is also inconsistent with the *initiation mechanism* 3. Following this initiation mechanism, the decay of DMEDA should have no induction period and should proceed independently regardless of the progress of the main chain reaction. Moreover, the formation of byproduct **3** could not be rationalized by this mechanism.[16] These contradictions prompted us to reconsider the radical initiation mechanism of the DMEDA/*t*-BuOK reaction system.

Investigating the Consumption of Diamine in the Cross-Coupling Reaction System. To collect sufficient experimental evidence for the radical initiation mechanism, it is essential to make clear how the diamine was consumed by characterization of its end-product(s). However, an attempt to identify DMEDA-related end-product failed, possibly due to its chemical lability. Therefore, we used *N*,*N*′-di-*tert*-butylethanediamine (D*t*BEDA) instead of DMEDA, expecting it to produce more stable end-product(s) for analysis due to the bulkier N-substituent. Prior work showed that D*t*BEDA was inactive in promoting the coupling reaction at 80 °C,[7a] but we found that it became an active promoter at slightly elevated temperature, enabling the end-product analysis (Table 1).

Table 1. Investigation into the End-Product of Diamine[a]

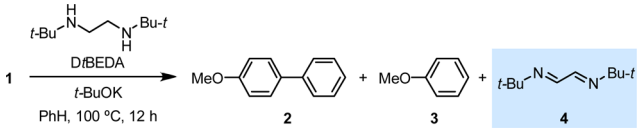

entry	D*t*BEDA loading (mol %)	conv. **1** (%)	GC yield (%) **2**	**3**	**4**[b]	D*t*BEDA[c]
1	0	11	6.7	1.0	–	–
2	20	27	17	2.8	4.2	95
3	100	81	47	25	9.9	81
4	300	94	39	51	6.8	92

[a]Reaction conditions: **1** (0.5 mmol), *t*-BuOK (1.5 mmol), D*t*BEDA (0–1.5 mmol), benzene (4 mL), sealed tube, 100 °C for 12 h. [b]Based on the amount of D*t*BEDA added. [c]Remaining D*t*BEDA after reaction.

It was observed that the conversion of **1** was raised as the loading of D*t*BEDA increased (entries 2–4), and control experiment showed only minor background reaction under 100 °C (entry 1). This clearly indicated that D*t*BEDA promoted the cross-coupling reaction like DMEDA, albeit less efficiently. Importantly, in all reactions performed with D*t*BEDA, diimine **4** was identified as the end-product (entries 2–4). This observation implied that in the diamine-promoted cross-coupling reaction, diamine was converted to the corresponding diimine, and the radical initiation process might relate to this transformation.

It is notable that the diamine to diimine transformation is an oxidation process with apparent loss of 4 electrons. Given that the cross-coupling reaction to produce biphenyl **2** is a redox-neutral process, while the generation of dehalogenation byproduct **3** from **1** is a reduction process demanding 2 electrons, it is reasonable to correlate the formation of byproduct **3** with the consumption of diamine. In the D*t*BEDA-promoted reactions, the yields of byproduct **3** were roughly twice as much as the yields of diimine **4** (Table 1); in the DMEDA-promoted reaction, the consumed DMEDA correlated with the amount of formed **3** in the reaction, showing a good linear relationship with a slop of ca. 2 (Figure 2). These are in agreement with the 2:1 stoichiometry of **3** to diamine calculated based on the number of electrons involved in the redox process.

Supported by the above results, it could be concluded that the conversion of DMEDA to diimine **5** took place in the model reaction system. We expected to reveal further details in this transformation to elucidate the radical initiation mechanism in the diamine/*t*-BuOK system.

Deuterium Labeling Experiments. To figure out how does the diamine to diimine conversion takes place in the reaction system, deuterium labeling experiments were conducted using the D*t*BEDA model (Table 2). Three deuterium-labeled diamines were prepared with deuterium substitution on the ethylene bridge (D*t*BEDA-d_4), the free NH group (D*t*BEDA-d_2), or both (D*t*BEDA-d_6). In general, deuterated diamines exhibited diminished activity and led to less dehalogenation byproduct **3** (Table 2, entries 1 and 2 vs Table 1, entries 3 and 4; Table 2, entries 3 and 4 vs Table 1, entry 4), but they were still able to promote the cross-coupling reaction. This was surprising because it is in contrast to the literature report that the ethylene bridge deuterated DMEDA had no activity.[12e] More importantly, the coupling reactions employing these deuterium-labeled diamines resulted in significant amount of deuterium incorporation at the

DOI: 10.1021/jacs.6b03442
J. Am. Chem. Soc. 2016, 138, 7151–7160

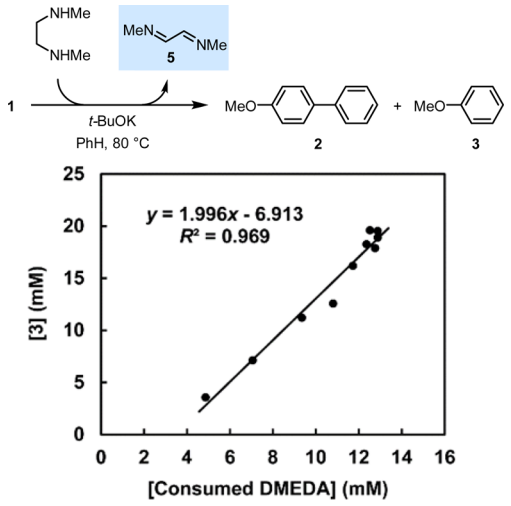

Figure 2. Plot for the correlation of DMEDA consumption with the generation of byproduct **3**, constructed from the data in Figure 1.

Table 2. Deuterium Labeling Experiments[a]

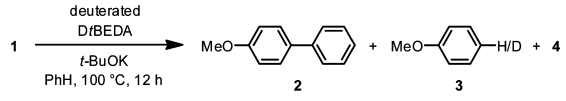

entry	deuterated DtBEDA	conv. 1 (%)	GC yield (%) 2	3[b]	4[c]	DtBEDA[d]
1	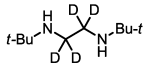 DtBEDA-d_4 (100 mol%)	51	38	10 (26% 4-D)	2.4	96
2	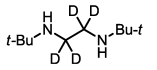 DtBEDA-d_4 (300 mol%)	89	47	36 (34% 4-D)	4.4	93
3	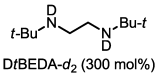 DtBEDA-d_2 (300 mol%)	80	34	36 (17% 4-D)	3.6	93
4	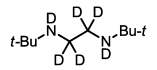 DtBEDA-d_6 (300 mol%)	80	50	25 (62% 4-D)	2.5	97

[a]Reaction conditions: **1** (0.5 mmol), *t*-BuOK (1.5 mmol), deuterium labeled DtBEDA (0.5 or 1.5 mmol), benzene (4 mL), sealed tube, 100 °C for 12 h. [b]Deuterium incorporation ratio of **3** was determined by GC–MS and ^{2}H NMR. [c]Based on the amount of DtBEDA added. [d]Remaining DtBEDA after reaction.

4-position of dehalogenation byproduct **3**, and the product distribution (**2**/**3**) varied with the deuterium-labeling pattern of diamine.

The deuterium labeling experiments on the DtBEDA model provided several key clues for the initiation mechanism. First, deuterium incorporation on C4-position of **3** clearly indicated a hydrogen atom transfer (HAT) process between the aryl radical and the diamine in the cross-coupling reaction, and verified the correlation between the formation of byproduct **3** and the consumption of diamine. Second, HAT occurred on either the ethylene bridge or the free NH groups of diamine, as demonstrated by the deuterium incorporation in **3** when DtBEDAs-d_4 and -d_2 were employed. Third, the radical initiation activity of the diamine/*t*-BuOK system was closely related to these HAT processes, because deuterated DtBEDAs exhibited diminished activities compared to normal DtBEDA. To date, HAT between aryl radical and the small molecule promoter and the remarkable effect of this process on the radical initiation activity were not taken into consideration in the diamine-promoted transition-metal-free cross-coupling reaction.

Kinetic Isotope Effect Study. To quantitatively assess the effect of deuterium substitution in diamine on its activity, the kinetic profiles of the model reaction employing deuterated diamines as promoters were acquired. Deuterated DMEDAs were used to perform kinetic study under unified reaction conditions (80 °C). Three deuterium-labeled DMEDAs were synthesized and employed to compare with normal DMEDA: DMEDA-d_4 with the ethylene bridge deuterated, DMEDA-d_6 with two *N*-methyl groups deuterated, and DMEDA-d_{10} with all C–H bonds deuterated (Figure 3). The results were quite

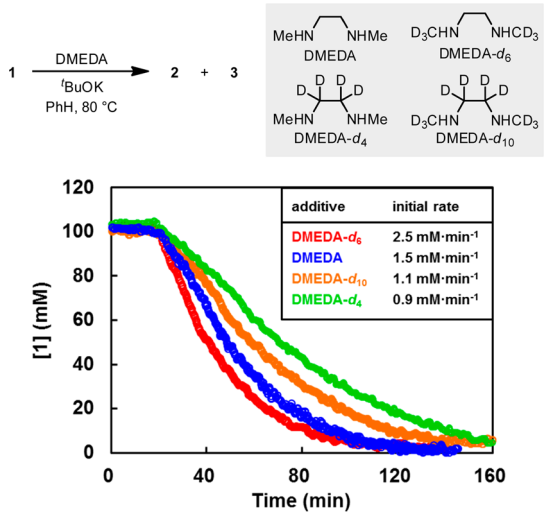

Figure 3. Time-adjusted kinetic profiles of [**1**] for the coupling reaction employing deuterated DMEDA as the additive. Reaction conditions: [**1**] = 100 mM, [*t*-BuOK] = 1.25 M, [DMEDA] = 20 mM, benzene as the solvent, 80 °C.

intriguing. First, all deuterated DMEDAs were able to promote the coupling reaction to full conversion in less than 3 h, again distinct from the previous report.[12e] Second, in these reactions, deuterium incorporation on the C4-position of byproduct **3** was observed for all deuterated DMEDAs, including the *N*-methyl deuterated DMEDA-d_6. Third, the activity of these molecules followed the order DMEDA-d_4 < DMEDA-d_{10} < DMEDA < DMEDA-d_6, in which *N*-methyl deuterated DMEDA-d_6 showed surprisingly high activity. This inverse KIE is unprecedented, indicating that HAT from the *N*-methyl group of DMEDA could also occur. Fourth, all reactions were found to have an induction period, and the duration of induction period for deuterated DMEDAs is considerably longer.

The present KIE study produced results in agreement with the deuterium-labeling experiments with DtBEDA. Taken together, we could conclude that the HAT process on diamine occurs not only on the ethylene bridge and the NH functionality, but also on the *N*-methyl groups. This accounts for the relatively low degree of deuteration in byproduct **3** when partially deuterated diamines were employed. The results also indicate that radical initiation in the diamine/*t*-BuOK system must operate differently from previously proposed, because all these experimental findings, including the kinetic profile, deuterium labeling experiment, and

DOI: 10.1021/jacs.6b03442
J. Am. Chem. Soc. 2016, 138, 7151–7160

the observed inverse KIE, could not be addressed by *initiation mechanism 3*. Since HAT between aryl radical and the diamine is found to be important and the activity of the reaction system is closely related to this process, the radical initiation process may stand as a mechanistic network involving a series of hydrogen atom transfer reactions, rather than a simple initiation pathway.

Mechanism for the Radical Initiation Process. At this stage, the above results could help to draw a new radical initiation mechanism for the DMEDA/*t*-BuOK system (Scheme 3). The process commences with HAT between aryl radical and DMEDA to afford dehalogenation product ArH. Hydrogen abstraction from the ethylene bridge leads to radical **IN1a**, and hydrogen abstraction from the NH group leads to **IN1b**. Although experimental results showed there was HAT from the *N*-methyl group, it does not occur at this step (according to DFT calculation results shown in Figure 7, vide infra). Deprotonation of both **IN1a** and **IN1b** by *t*-BuOK leads to radical anion **IN2** (a potent electron donor), which then undergoes SET to the aryl iodide substrate to regenerate an aryl radical together with monoimine **IN3**. The initiation process bifurcates at this point. Following pathway 1, **IN3** undergoes a second HAT with aryl radical to produce byproduct ArH and radical intermediates **IN4a** and **IN4b**. HAT from the methylene of **IN3** leads to **IN4a**, while HAT from the *N*-Me on the secondary amine of **IN3** leads to **IN4b**. HAT from the imine *N*-Me is disfavored (according to DFT calculation). Following pathway 2, **IN3** is deprotonated by *t*-BuOK to form enamide **IN5**, which serves as an electron donor to undergo SET to the ArI substrate, producing a new aryl radical, as well as radical **IN4a**. The two pathways converge at radical **IN4a**, which is further deprotonated to form radical anion **IN6a**. Finally, **IN6a** undergoes SET to the ArI substrate and produces diimine **5**. It is reasonable to assume that the fate of **IN4b** is similar to that of **IN4a**, in which deprotonation and SET generate a new aryl radical as well as diimine **6**. In the proposed initiation mechanism, all deprotonation steps are thought to be irreversible, because *t*-BuOH was found to have no inhibitory effect on the reaction (see the Supporting Information for details).

Scheme 3. Proposed Radical Initiation Network for the DMEDA/*t*-BuOK Reaction System

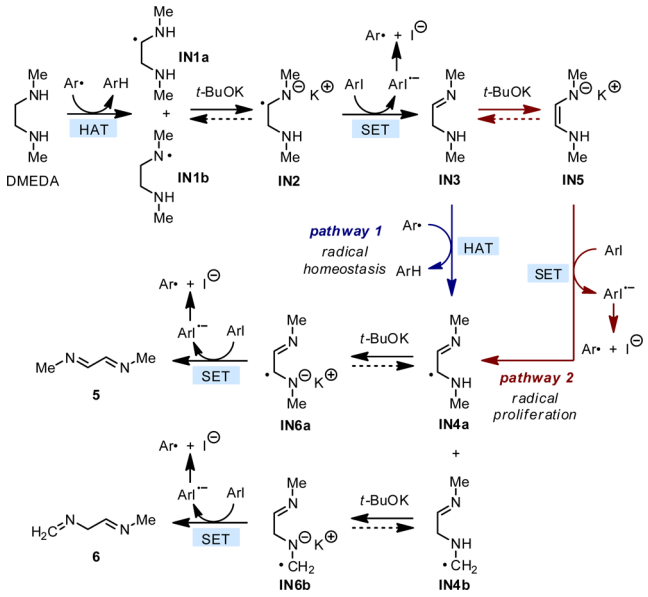

The mechanistic network of radical initiation is consistent with the nonindependent consumption kinetics of diamine (Figure 1), and well accounts for the observed 1:2 stoichiometry between diamine and byproduct **3** (Figure 2). Moreover, this network showcases the interesting function of diamine to regulate the radical concentration. Following pathway 1 (DMEDA → **IN3** → **IN4a/b** → **5/6**, referred to as *radical homeostasis pathway*), two aryl radicals are consumed and two are regenerated, resulting in no net change in aryl radical count. On the other hand, following pathway 2 (DMEDA → **IN3** → **IN5** → **IN4a** → **5**, referred to as *radical proliferation pathway*), one aryl radical is consumed and three are regenerated, leading to aryl radical proliferation. Under low [Ar·], the radical proliferation pathway predominates and the DMEDA/*t*-BuOK system acts as a powerful "radical amplifier"; under high [Ar·], the radical homeostasis pathway becomes more important to maintain dynamic balance of the aryl radical concentration. In the early stage of the reaction, trace amount of the initial aryl radical could be generated by the background reaction, as demonstrated by the control experiments (Table 1, entry 1)[17] and the literature report.[12c] According to the proposed radical initiation network, this trace amount of aryl radical triggers the aryl radical proliferation in the DMEDA/*t*-BuOK reaction system following pathway 2, which accounts for the induction period observed in the kinetic study.

Experimental Evidence for the Initiation Mechanism. Several experiments were performed to provide further support for the proposed initiation mechanism. First, the nature of some redox-active species involved in the initiation process was evaluated by electrochemical study. We sought to characterize the electron-donating ability of some proposed electron donors involved in SET process. To this end, the reduction potentials of monoimine complex **7**[18] (analogue of **IN3**) and diimine **4** (analogue of **5**) were determined (Figure 4). The result, E_{red}(**7**) = −2.1 V and E_{red}(**4**) = −2.0 V vs $Fc^{+/0}$, suggests that the oxidation potentials of the proposed electron donors, **IN2** and **IN6a**, are close to −2.0 V. The small potential gap ($\Delta E \approx 0.9$ V) between the oxidation of these electron donors and the reduction of iodoarene **1** provides support for the SET processes in the proposed initiation mechanism.

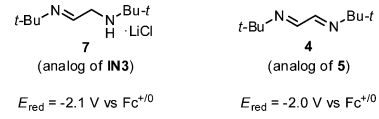

Figure 4. Reduction potentials for the analogues of key redox-active species measured by differential pulse voltammetry (DPV).

Second, the crucial role of intermediate **IN3**, the bifurcation point in the proposed mechanism, was confirmed by independent experiment with its analogue, compound **7**. It was found that monoimine **7** alone could promote the model coupling reaction, producing the coupling product **2** in 57% yield together with 15% yield of **3** (Figure 5). Diimine **4** was detected in significant amount as the end-product of **7**, which is in line with the proposed initiation pathways **IN3** → **5**. Notably, as demonstrated by operando IR spectroscopy, the reaction promoted by monoimine **7** exhibited no induction period, which is distinct from the reaction promoted by DMEDA (Figure 5). This provides support for the proposed initiation mechanism, in which monoimine **IN3** directly enables the radical proliferation pathway (Scheme 3).

DOI: 10.1021/jacs.6b03442
J. Am. Chem. Soc. 2016, 138, 7151−7160

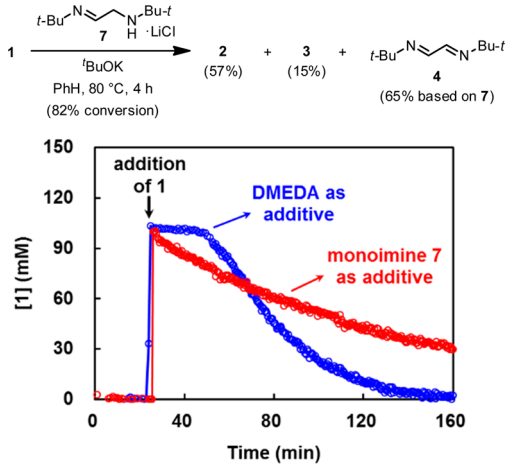

Figure 5. Time-adjusted kinetic profiles of [**1**] for the coupling reaction employing DMEDA (blue) and monoimine **7** (red) as the additive. Reaction conditions: [**7**] = 22 mM, [**1**] = 100 mM, [*t*-BuOK] = 1.25 M, benzene as the solvent, 80 °C.

Third, it was found that, by addition of trace amount of iodine to the reaction system, the induction period was remarkably shortened and acceleration of the reaction was observed. The magnitude of this positive effect depends on the amount of iodine added: addition of 0.2 mol % I_2 resulted in initiation of the reaction within 1 min without interfering with the reaction kinetics (Figure S12), while addition of 1−2 mol % I_2 initiated the reaction immediately and led to reaction acceleration (Figure 6). Control experiment revealed that I_2 alone (without diamine)

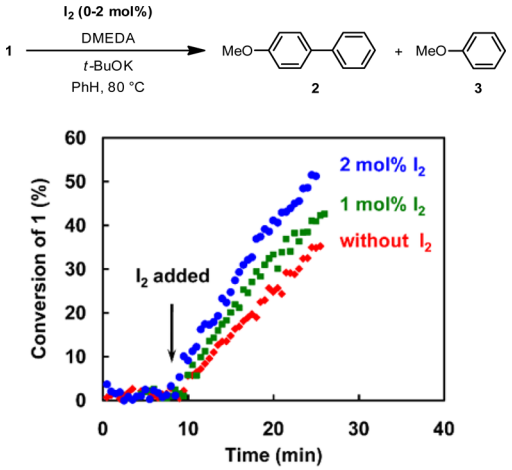

Figure 6. Time-adjusted plot of the conversion of **1** in the model reaction with different amount of I_2 added. Reaction conditions: [**1**] = 100 mM, [DMEDA] = 20 mM, [*t*-BuOK] = 1.25 M, benzene as the solvent, 80 °C.

could not initiate the reaction. Given that I_2 could convert an amine to imine,[19] this iodine initiation experiment provides support for the proposed initiation mechanism: DMEDA could be oxidized to monoimine **IN3** by the added I_2, and **IN3** initiates the reaction easily.

Finally, observations in our deuterium labeling experiments and the KIE study also strongly support the proposed radical initiation network. Deuteration on ethylene bridge and amine NH group of the diamine makes it less effective in initiating the coupling reaction, because primary kinetic isotope effect would result in a higher barrier for HAT. In contrast, deuteration on the *N*-Me groups of DMEDA slows down the **IN3** → **IN4b** process and thus increases the steady state concentration of **IN3**, which favors the radical proliferation pathway. This is in agreement with the observation that *N*-Me deuterated DMEDAs exhibited a better activity compared with DMEDAs without *N*-Me deuteration (a quantitative understanding of this phenomenon is shown later).

Computational Study. Density functional theory (DFT) computational study[20] was conducted to confirm the proposed initiation mechanistic network. The reactions depicted in Scheme 3 were calculated at the M06-2X[21]/6-311+G(d,p) level of theory using the CPCM method to evaluate the solvation effect in benzene, in which phenyl group was used as the Ar substituent. The potential energy surface was established based on calculated Gibbs free energies in benzene (Figure 7).

It was found that HAT between phenyl radical (Ph·) and DMEDA could occur at two positions: hydrogen abstraction from the ethylene bridge via **TS1a** produces carbon-centered radical **IN1a** with an activation barrier of 11.4 kcal/mol; hydrogen abstraction from the NH group via **TS1b** produces nitrogen-centered radical **IN1b** with slightly elevated activation barrier, 11.8 kcal/mol. HAT from the *N*-Me group of DMEDA via **TS1c** has a greater activation barrier (14.5 kcal/mol) and is not feasible. Radical intermediates **IN1a** and **IN1b** then undergo proton abstraction with *t*-BuOK via **TS2a** and **TS2b**, respectively, to afford the same intermediate **IN2′**, which has the feature of a radical anion and serves as an electron donor. Subsequent SET between **IN2′** and iodobenzene (PhI) to form iodobenzene radical anion/*t*-BuOH complex **IN7** and monoimine **IN3** is exergonic by 16.5 kcal/mol, rendering the overall process (**IN1a**/**1b** → **IN3**) thermodynamically favored. The initiation network bifurcates at **IN3**. Following pathway 1, a second HAT occurs between Ph· and the methylene group in **IN3** to form radical **IN4a** via **TS3a** with an activation energy barrier of 11.5 kcal/mol. The following proton abstraction by *t*-BuOK afforded intermediate **IN6a′**. The electron transfer between **IN6a′** and PhI to form **IN7** and diimine **5** is endergonic by 7.8 kcal/mol, but subsequent C−I bond cleavage of **IN7** makes the overall process exergonic by 6.2 kcal/mol. A parallel route in pathway 1, in which HAT between Ph· and **IN3** occurs at the *N*-Me of the secondary amine via **TS3b**, is also evaluated by DFT calculation. This event produces radical **IN4b**, which then undergoes deprotonation and electron transfer to form diimine **6** resembling **IN4a**. Although this route has a higher activation energy barrier compared with HAT from the methylene in **IN3** (12.3 vs 11.5 kcal/mol), it is important because it accounts for the experimentally observed HAT from the *N*-Me group of DMEDA. These two parallel routes constitute pathway 1 and they proceed simultaneously. In pathway 2, deprotonation of **IN3** by *t*-BuOK via **TS5** to form enamide **IN5′** is endergonic by 11.4 kcal/mol with an activation energy barrier of 14.9 kcal/mol. SET from **IN5′** to PhI is endergonic by 12.8 kcal/mol, producing radical **IN4a** and iodobenzene radical anion/*t*-BuOH complex **IN7**. In conjugation with subsequent C−I bond cleavage, this process is slightly exergonic by 1.2 kcal/mol. Then, **IN4a** could be further converted to diimine **5** following pathway 1. The potential energy surface indicates that pathway 1 is favored over pathway 2 when sufficient concentration of aryl radical is present.

The calculated potential energy surface is in good agreement with all experimental observations and provides support for the proposed mechanism: (i) the HAT processes between aryl radical and DMEDA could occur on multiple sites of the diamine

DOI: 10.1021/jacs.6b03442
J. Am. Chem. Soc. 2016, 138, 7151−7160

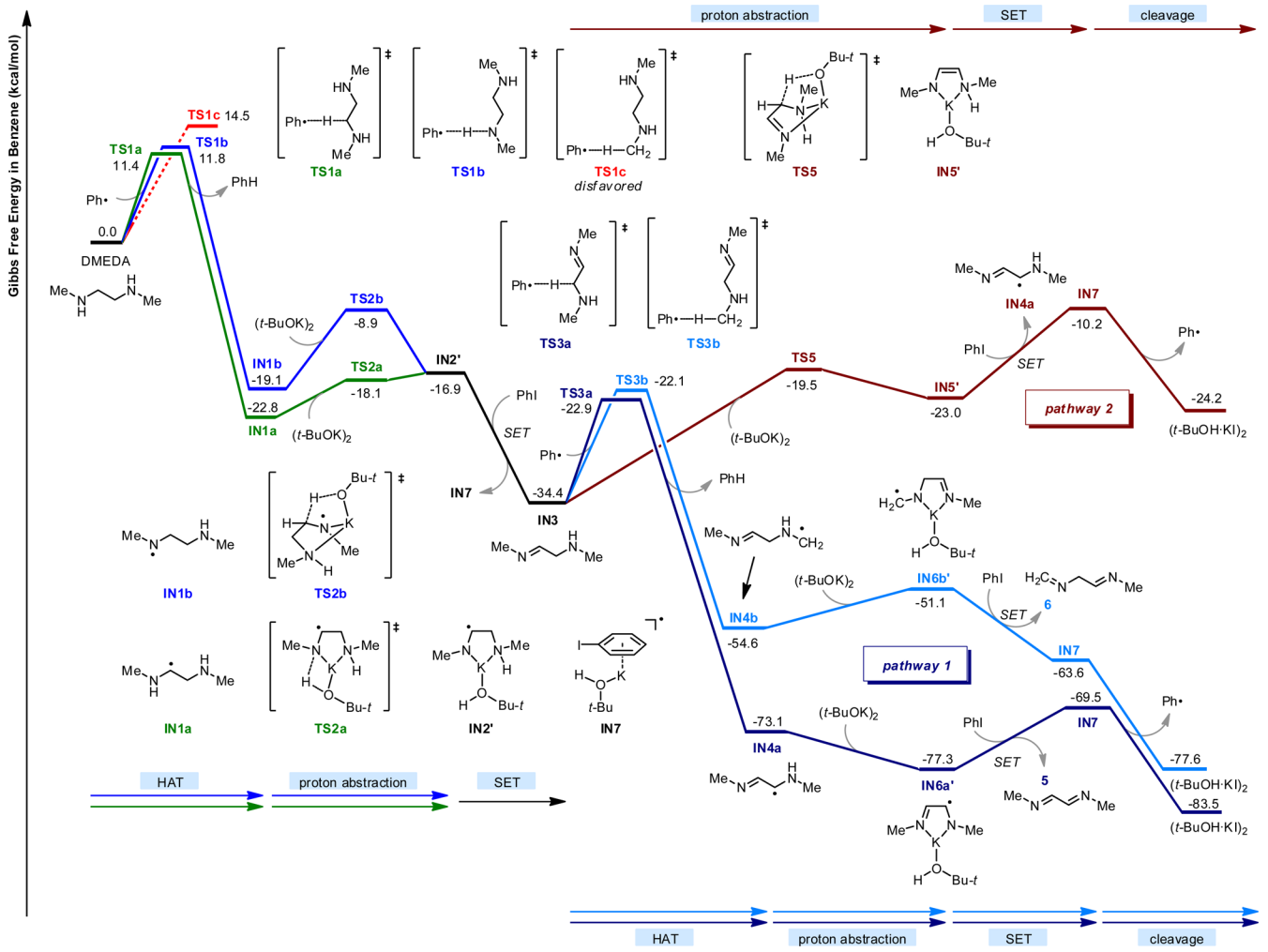

Figure 7. Gibbs free energy ($\Delta G_{\text{solv 298K}}$) profile for the initiation pathways calculated at the M06-2X/6-311+G(d,p) level of theory.

and are feasible both thermodynamically and kinetically; (ii) the electron-rich intermediates (**IN2′**, **IN6a′**, **IN6b′**, and **IN5′**, correspond to **IN2**, **IN6**, and **IN5** in Scheme 3) are able to undergo SET with the aryl iodide; (iii) the initiation pathways and the main chain reaction proceed simultaneously, because the activation barriers of HAT (between aryl radical and DMEDA) and radical addition (between aryl radical and benzene) are similar (11.4/11.8 vs 15.2 kcal/mol).[22] Although the HAT process is more facile than radical addition as judged by $\Delta G^{\ddagger}$, the low concentration of DMEDA (ca. 20 mM) and high concentration of benzene (as solvent) make the main chain reaction favored.

Kinetic Studies. In addition to DFT calculation, reaction kinetics provided important support for this radical initiation network. Bringing the proposed initiation mechanism and the main chain reaction together, a kinetic model for the complete DMEDA/*t*-BuOK reaction system is established (Scheme 4). The model comprises two parts, the initiation network and the cross-coupling part, where chain initiation and propagation steps were included, respectively. The chain termination pathway is assumed to be the homocoupling of the reactive aryl radical, which has a bimolecular rate constant of $>10^9$ $M^{-1}\cdot s^{-1}$.[23]

Although this kinetic model seems complicated, clear and simple rate laws could be derived by applying steady-state approximation to all reactive intermediates.[24] Solving for the concentration of the key radical species, [Ar·], one obtains:

$$[\text{Ar}\cdot] = \frac{\sqrt{k_t^{\,2}k_2^{\,2}[t\text{-BuOK}]^2 + 4k_{\text{HAT1}}k_{\text{HAT2}}k_tk_2[t\text{-BuOK}][\text{DMEDA}]} - k_tk_2[t\text{-BuOK}]}{2k_{\text{HAT2}}k_t} \quad (1)$$

The rate laws for aryl iodide consumption and product formation are

$$-\frac{\text{d}[\text{ArI}]}{\text{d}t} \approx k_{\text{add}}[\text{PhH}][\text{Ar}\cdot] + 2k_{\text{HAT1}}[\text{DMEDA}][\text{Ar}\cdot] \quad (2)$$

$$\frac{\text{d}[\text{ArPh}]}{\text{d}t} = k_{\text{add}}[\text{PhH}][\text{Ar}\cdot] \quad (3)$$

$$\frac{\text{d}[\text{ArH}]}{\text{d}t} \approx 2k_{\text{HAT1}}[\text{DMEDA}][\text{Ar}\cdot] \quad (4)$$

DOI: 10.1021/jacs.6b03442
J. Am. Chem. Soc. 2016, 138, 7151−7160

Scheme 4. Kinetic Model for the DMEDA/*t*-BuOK Cross-Coupling Reaction System

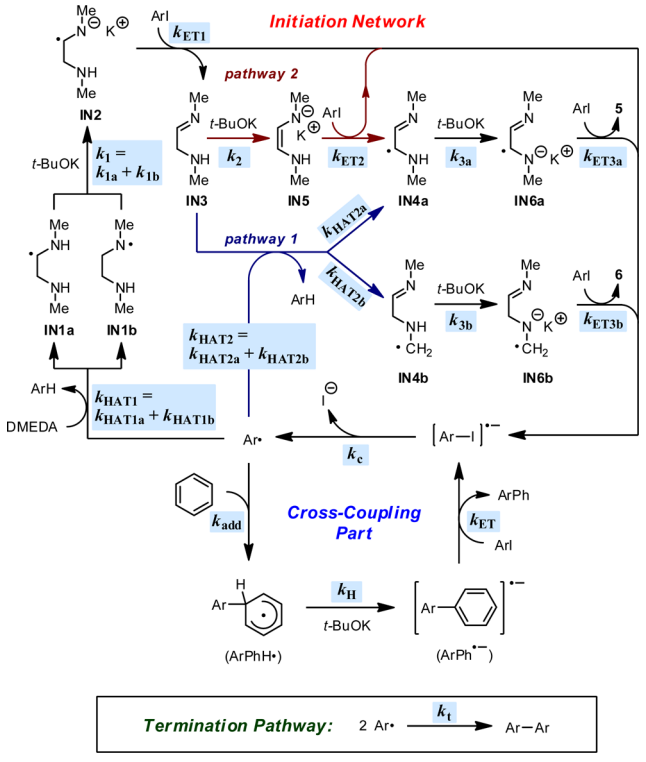

Substitution of eq 1 into eqs 2−4 and treating [PhH] as constant give the simplified rate laws:

$$-\frac{\mathrm{d[ArI]}}{\mathrm{d}t} \approx (1 + c[\mathrm{DMEDA}])\cdot (\sqrt{a^2[t\text{-BuOK}]^2 + b[t\text{-BuOK}][\mathrm{DMEDA}]} - a[t\text{-BuOK}]) \quad (5)$$

$$\frac{\mathrm{d[ArPh]}}{\mathrm{d}t} = \sqrt{a^2[t\text{-BuOK}]^2 + b[t\text{-BuOK}][\mathrm{DMEDA}]} - a[t\text{-BuOK}] \quad (6)$$

$$\frac{\mathrm{d[ArH]}}{\mathrm{d}t} \approx c[\mathrm{DMEDA}]\cdot (\sqrt{a^2[t\text{-BuOK}]^2 + b[t\text{-BuOK}][\mathrm{DMEDA}]} - a[t\text{-BuOK}]) \quad (7)$$

where a, b, and c are constants composed of various rate constants:

$$a = \frac{k_2 k_{\mathrm{add}}[\mathrm{PhH}]}{2k_{\mathrm{HAT2}}} \quad (8)$$

$$b = \frac{k_{\mathrm{HAT1}} k_2 {k_{\mathrm{add}}}^2 [\mathrm{PhH}]^2}{k_{\mathrm{HAT2}} k_{\mathrm{t}}} \quad (9)$$

$$c = \frac{2k_{\mathrm{HAT1}}}{k_{\mathrm{add}}[\mathrm{PhH}]} \quad (10)$$

These rate laws reveal explicit relationships between the reaction kinetics and the concentrations of both DMEDA and *t*-BuOK. Aiming to verify the radical initiation mechanism, kinetic analysis was performed for the model reaction. A series of initial rate experiments were conducted to establish the dependence of reaction rate on each component. It was found that the initial rate based on consumption of **1** exhibited zero-order in [**1**], in accordance with eq 5 that no term relates to [**1**] exists in the rate law. The reaction rate showed positive orders in both [DMEDA] and [*t*-BuOK], which was in agreement with eq 5. Gratifyingly, the measured rate dependence fit very well to eq 5 (Figure 8), indicating that the reaction kinetics is subject to the rate law derived from the present kinetic model.

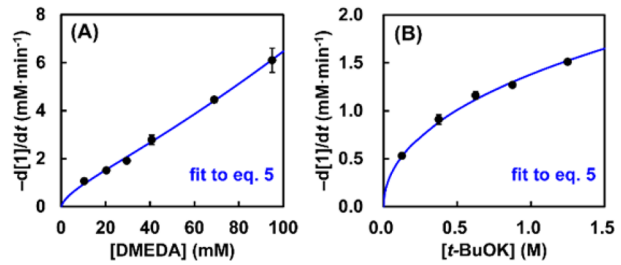

Figure 8. Dependence of the initial rate on [DMEDA] (A) and [*t*-BuOK] (B). Reaction conditions: (A) [DMEDA] = 10−100 mM, [**1**] = 100 mM, [*t*-BuOK] = 1.25 M; (B) [*t*-BuOK] = 0.125−1.25 M, [**1**] = 100 mM, [DMEDA] = 20 mM; benzene as the solvent, 80 °C.

Furthermore, comparison between eqs 6 and 7 shows that, following the proposed mechanism, the generation of byproduct ArH (**3**) is more directly related to [DMEDA] than product ArPh (**2**). By dividing eq 7 with eq 6, a simple linear relationship between [ArH] to [ArPh] ratio and [DMEDA] emerged:

$$\left.\frac{[\mathrm{ArH}]}{[\mathrm{ArPh}]}\right|_{\mathrm{initial}} = \frac{\mathrm{d[ArH]}/\mathrm{d}t}{\mathrm{d[ArPh]}/\mathrm{d}t} = c[\mathrm{DMEDA}] \quad (11)$$

Thus, the model reactions with different [DMEDA] were performed and the [**3**]/[**2**] ratios were determined at low conversion (<30%). It was found that the [**3**]/[**2**] ratio exhibited a good linear relationship with [DMEDA] (Figure 9), which is in good agreement with eq 11 and demonstrates the importance of DMEDA in the HAT process.

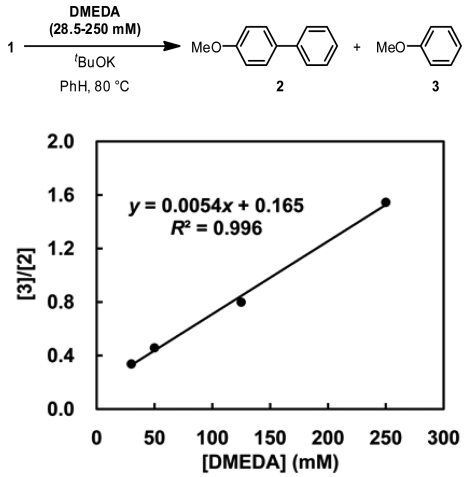

Figure 9. Relationship between the ratio of anisole (**3**) to product (**2**) and [DMEDA]. Reaction conditions: [**1**] = 100 mM, [DMEDA] = 28.5−250 mM, [*t*-BuOK] = 1.25 M, benzene as the solvent, 80 °C.

DOI: 10.1021/jacs.6b03442
J. Am. Chem. Soc. 2016, 138, 7151−7160

Finally, the inverse kinetic isotope effect observed for *N*-Me deuterated DMEDAs (Figure 3) could be well rationalized by the derived rate laws. Because deuterium substitution on *N*-Me group of DMEDA does not affect HAT on the ethylene bridge and the NH group, DMEDA-d_6 exhibits the same rate constant k_{HAT1} as normal DMEDA. However, in pathway 1, rate constant for HAT on the *N*-Me group of **IN3**, k_{HAT2b}, will decrease dramatically due to primary KIE. Therefore, the DMEDA-d_6/*t*-BuOK reaction system has the same k_{HAT1} but decreased k_{HAT2} compared with DMEDA/*t*-BuOK system. From a mathematic point of view, in the rate laws the term k_{HAT2} always exists in denominator (eqs 5−10); thus, a smaller k_{HAT2} results in a greater reaction rate. From a mechanistic viewpoint, the slower HAT in pathway 1 leads to a higher steady-state concentration of **IN3** in the chain process, which subsequently results in an accelerated radical proliferation pathway 2. The observation that DMEDA-d_{10} is more active than DMEDA-d_4 could be rationalized by the same principle. This intriguing inverse kinetic isotope effect is difficult to understand without considering this initiation network.

Detailed kinetic analysis showed that the features of the DMEDA/*t*-BuOK reaction system perfectly matched those predicted from the kinetic model. This provides important support for the proposed radical initiation network.

CONCLUSION

In this article, the DMEDA/*t*-BuOK reaction system was selected as a representative model to study the unusual radical initiation mechanism in transition-metal-free cross-coupling reactions developed in recent years. Through a combined experimental and DFT computational study, the radical initiation mechanism in the diamine-promoted cross-coupling reaction was carefully reinvestigated. The results revealed an unconventional radical initiation network in the DMEDA/*t*-BuOK system, which could replace the previously proposed radical initiation mechanism.

The key question regarding the initiation mechanism is the role of diamine in the reaction. Preliminary kinetic study excluded the role of DMEDA as a catalyst or a radical initiator, and ruled out the simple redox-type initiation pathway proposed in previous study. End-product analysis, deuterium labeling experiments, KIE study, electrochemical study, intermediate synthesis, and initiation experiments suggested a novel radical initiation mechanistic network involving hydrogen atom transfer between DMEDA and the aryl radical. In this network, the diamine does not directly promote the generation of aryl radical, but plays a dual role: first, it enables proliferation of the initial aryl radical to initiate the radical chain reaction (as a radical amplifier); second, it regulates the concentration of the aryl radical by HAT-based processes (as a radical regulator). This has been further verified by DFT calculation and kinetic analysis. In particular, kinetic analysis was performed on the transition-metal-free cross-coupling reaction for the first time, which provided significant support for the reaction mechanism. Interestingly, the revealed radical initiation network is more complicated than the main chain reaction. This mechanistic network and the subtle role of such simple diamine molecule in the radical chain reaction are rather uncommon.

The present study sheds some light on the novel radical initiation mechanism of the transition-metal-free cross-coupling reactions promoted by small molecule organic additives. Previously, it was thought that aryl radical only participates in the main chain reaction to produce the cross-coupling product. The discovery that aryl radical could also interact with the small molecule promoter and thus modulate the activity of the reaction system represents a novel and unprecedented radical initiation mode, which would be taken into account when studying related reactions. Also, as learned from this study, a hydrogen atom donor moiety with a neighboring X—H bond might be the key structural feature of a successful promoter that efficiently initiates the transition-metal-free coupling reaction. Diols, aminoalcohols, alkyl alcohols, hydrazine derivatives, and amino acids fall into this category and were all proved to be efficient promoters in this reaction. We expect the insight obtained from this study to help to understand the mechanism of many relevant reactions, as well as to guide the development of more efficient radical chain reactions for synthesis.

ASSOCIATED CONTENT

Supporting Information

The Supporting Information is available free of charge on the ACS Publications website at DOI: 10.1021/jacs.6b03442.

Experimental procedures, kinetic data, details for rate law deduction, and computational results (PDF)

AUTHOR INFORMATION

Corresponding Author

*Leijiao@mail.tsinghua.edu.cn

Notes

The authors declare no competing financial interest.

ACKNOWLEDGMENTS

The Thousand Talents Plan for Young Professionals and the National Natural Science Foundation of China (Grant No. 21390403) are acknowledged for financial support. We thank Prof. Ming-Tian Zhang for helpful discussions and suggestions. The technology platform of CBMS and the Tsinghua Xuetang Talents Program are acknowledged for providing instrumentation and computational resources.

REFERENCES

(1) (a) Perkins, M. J. *Radical Chemistry: The Fundamentals*; Oxford University Press: Oxford, 2000. (b) Zard, S. Z. *Radical Reactions in Organic Synthesis*; Oxford University Press: Oxford, 2003. (c) Togo, H. *Advanced Free Radical Reactions for Organic Synthesis*; Elsevier: Amsterdam, 2004. (d) Todres, Z. V. *Ion-Radical Organic Chemistry: Principles and Applications*, 2nd ed.; CRC Press: Boca Raton, FL, 2009. (e) *Encyclopedia of Radicals in Chemistry, Biology and Materials*; Chatgilialoglu, C., Studer, A., Eds.; Wiley: New York, 2012.

(2) (a) Jasperse, C. P.; Curran, D. P.; Fevig, T. L. *Chem. Rev.* **1991**, *91*, 1237−1286. (b) Motherwell, W. B.; Crich, D. *Free Radical Chain Reactions in Organic Synthesis*; Katritzky, A. R., Meth-Cohn, O., Rees, C. S., Eds.; Academic Press Limited: London, 1992. (c) Zimmerman, J.; Sibi, M. P. *Top. Curr. Chem.* **2006**, *263*, 107−162. (d) Albert, M.; Fensterbank, L.; Lacôte, E.; Malacria, M. *Top. Curr. Chem.* **2006**, *264*, 1−62. (e) Walton, J. C. *Top. Curr. Chem.* **2006**, *264*, 163−200.

(3) (a) Denisov, E. T.; Denisova, T. G.; Pokidova, T. S. *Handbook of Free Radical Initiators*; Wiley: Hoboken, NJ, 2003. (b) Lalevée, J.; Fouassier, J. P. In *Encyclopedia of Radicals in Chemistry, Biology and Materials*; Chatgilialoglu, C., Studer, A., Eds.; Wiley: New York, 2012; pp 37−56.

(4) Yanagisawa, S.; Ueda, K.; Taniguchi, T.; Itami, K. *Org. Lett.* **2008**, *10*, 4673−4676.

(5) For reviews, see: (a) Yanagisawa, S.; Itami, K. *ChemCatChem* **2011**, *3*, 827−829. (b) Pan, S. C. *Beilstein J. Org. Chem.* **2012**, *8*, 1374−1384. (c) Wang, L.; Yan, G.; Zhang, X. *Youji Huaxue* **2012**, *32*, 1864−1871. (d) Chan, T. L.; Wu, Y.; Choy, P. Y.; Kwong, F. Y. *Chem. - Eur. J.* **2013**,

DOI: 10.1021/jacs.6b03442
J. Am. Chem. Soc. 2016, 138, 7151−7160

19, 15802−15814. (e) Mehta, V. P.; Punji, B. *RSC Adv.* **2013**, *3*, 11957−11986. (f) Sun, C.-L.; Shi, Z.-J. *Chem. Rev.* **2014**, *114*, 9219−9280.

(6) For recent reviews and books on transition-metal-catalyzed cross-coupling reactions, see: (a) Alberico, D.; Scott, M. E.; Lautens, M. *Chem. Rev.* **2007**, *107*, 174−238. (b) Chen, X.; Engle, K. M.; Wang, D.-H.; Yu, J.-Q. *Angew. Chem., Int. Ed.* **2009**, *48*, 5094−5115. (c) *Modern Arylation Methods*; Ackermann, L., Ed.; Viley-VCH: Weinheim, 2009. (d) Lyons, T. W.; Sanford, M. S. *Chem. Rev.* **2010**, *110*, 1147−1169. (e) Lei, A.; Liu, W.; Liu, C.; Chen, M. *Dalton Trans.* **2010**, *39*, 10352−10361. (f) Jana, R.; Pathak, T. P.; Sigman, M. S. *Chem. Rev.* **2011**, *111*, 1417−1492. (g) *Metal-Catalyzed Cross-Coupling Reactions and More*; de Meijere, A., Bräse, S., Oestereich, M., Eds.; Wiley-VCH: Weinheim, 2014.

(7) For intermolecular cross-coupling reactions, see: (a) Liu, W.; Cao, H.; Zhang, H.; Zhang, H.; Chung, K. H.; He, C.; Wang, H.; Kwong, F. Y.; Lei, A. *J. Am. Chem. Soc.* **2010**, *132*, 16737−16740. (b) Sun, C.-L.; Li, H.; Yu, D.-G.; Yu, M.; Zhou, X.; Lu, X.-Y.; Huang, K.; Zheng, S.-F.; Li, B.-J.; Shi, Z.-J. *Nat. Chem.* **2010**, *2*, 1044−1049. (c) Shirakawa, E.; Itoh, K.-i.; Higashino, T.; Hayashi, T. *J. Am. Chem. Soc.* **2010**, *132*, 15537−15539. (d) Qiu, Y.; Liu, Y.; Yang, K.; Hong, W.; Li, Z.; Wang, Z.; Yao, Z.; Jiang, S. *Org. Lett.* **2011**, *13*, 3556−3559. (e) Yong, G.-P.; She, W.-L.; Zhang, Y.-M.; Li, Y.-Z. *Chem. Commun.* **2011**, *47*, 11766−11768. (f) Tanimoro, K.; Ueno, M.; Takeda, K.; Kirihata, M.; Tanimori, S. *J. Org. Chem.* **2012**, *77*, 7844−7849. (g) Liu, H.; Yin, B.; Gao, Z.; Li, Y.; Jiang, H. *Chem. Commun.* **2012**, *48*, 2033−2035. (h) Chen, W.-C.; Hsu, Y.-C.; Shih, W.-C.; Lee, C.-Y.; Chuang, W.-H.; Tsai, Y.-F.; Chen, P. P.-Y.; Ong, T.-G. *Chem. Commun.* **2012**, *48*, 6702−6704. (i) Ng, Y. S.; Chan, C. S.; Chan, K. S. *Tetrahedron Lett.* **2012**, *53*, 3911−3914. (j) A, S.; Liu, X.; Li, H.; He, C.; Mu, Y. *Asian J. Org. Chem.* **2013**, *2*, 857−861. (k) Zhao, H.; Shen, J.; Guo, J.; Ye, R.; Zeng, H. *Chem. Commun.* **2013**, *49*, 2323−2325. (l) Liu, W.; Tian, F.; Wang, X.; Yu, H.; Bi, Y. *Chem. Commun.* **2013**, *49*, 2983−2985. (m) Li, B.; Qin, X.; You, J.; Cong, X.; Lan, J. *Org. Biomol. Chem.* **2013**, *11*, 1290−1293. (n) Dewanji, A.; Murarka, S.; Curran, D. P.; Studer, A. *Org. Lett.* **2013**, *15*, 6102−6105. (o) Sharma, S.; Kumar, M.; Kumar, V.; Kumar, N. *Tetrahedron Lett.* **2013**, *54*, 4868−4871. (p) Song, Q.; Zhang, D.; Zhu, Q.; Xu, Y. *Org. Lett.* **2014**, *16*, 5272−5274. (q) Ghosh, D.; Lee, J.-Y.; Liu, C.-Y.; Chiang, Y.-H.; Lee, H. M. *Adv. Synth. Catal.* **2014**, *356*, 406−410. (r) Zhu, Y.-W.; Yi, W.-B.; Qian, J.-L.; Cai, C. *ChemCatChem* **2014**, *6*, 733−735. (s) Cuthbertson, J.; Gray, V. J.; Wilden, J. D. *Chem. Commun.* **2014**, *50*, 2575−2578. (t) Bhakuni, B. S.; Yadav, A.; Kumar, S.; Kumar, S. *New J. Chem.* **2014**, *38*, 827−836. (u) Wu, Y.; Choy, P. Y.; Kwong, F. Y. *Org. Biomol. Chem.* **2014**, *12*, 6820−6823. (v) Liu, W.; Xu, L.; Bi, Y. *RSC Adv.* **2014**, *4*, 44943−44947. (w) Liu, W.; Liu, R.; Bi, Y. *Tetrahedron* **2015**, *71*, 2622−2628. (x) Gao, Y.; Tang, P.; Zhou, H.; Zhang, W.; Yang, H.; Yan, N.; Hu, G.; Mei, D.; Wang, J.; Ma, D. *Angew. Chem., Int. Ed.* **2016**, *55*, 3124−3128. (y) Paira, R.; Singh, B.; Hota, P. K.; Ahmed, J.; Sau, S. C.; Johnpeter, J. P.; Mandal, S. K. *J. Org. Chem.* **2016**, *81*, 2432−2441.

(8) For intramolecular cross-coupling reactions, see: (a) Sun, C.-L.; Gu, Y.-F.; Huang, W.-P.; Shi, Z.-J. *Chem. Commun.* **2011**, *47*, 9813−9815. (b) Roman, D. S.; Takahashi, Y.; Charette, A. B. *Org. Lett.* **2011**, *13*, 3242−3245. (c) Bhakuni, B. S.; Kumar, A.; Balkrishna, S. J.; Sheikh, J. A.; Konar, S.; Kumar, S. *Org. Lett.* **2012**, *14*, 2838−2841. (d) De, S.; Ghosh, S.; Bhunia, S.; Sheikh, J. A.; Bisai, A. *Org. Lett.* **2012**, *14*, 4466−4469. (e) Wu, Y.; Wong, S. M.; Mao, F.; Chan, T. L.; Kwong, F. Y. *Org. Lett.* **2012**, *14*, 5306−5309. (f) Masters, K.-S.; Bräse, S. *Angew. Chem., Int. Ed.* **2013**, *52*, 866−869. (g) De, S.; Mishra, S.; Kakde, B. N.; Dey, D.; Bisai, A. *J. Org. Chem.* **2013**, *78*, 7823−7844.

(9) For photoirradiation-induced cross-coupling, see: (a) Budén, M. E.; Guastavino, J. F.; Rossi, R. A. *Org. Lett.* **2013**, *15*, 1174−1177. (b) Cheng, Y.; Gu, X.; Li, P. *Org. Lett.* **2013**, *15*, 2664−2667. (c) Zheng, X.; Yang, L.; Du, W.; Ding, A.; Guo, H. *Chem. - Asian J.* **2014**, *9*, 439−442. (d) Kawamoto, T.; Sato, A.; Ryu, I. *Org. Lett.* **2014**, *16*, 2111−2113. (e) Xu, Z.; Gao, L.; Wang, L.; Gong, M.; Wang, W.; Yuan, R. *ACS Catal.* **2015**, *5*, 45−50.

(10) For Heck-type reactions, see: (a) Shirakawa, E.; Zhang, X.; Hayashi, T. *Angew. Chem., Int. Ed.* **2011**, *50*, 4671−4674. (b) Sun, C.-L.; Gu, Y.-F.; Wang, B.; Shi, Z.-J. *Chem. - Eur. J.* **2011**, *17*, 10844−10847. (c) Rueping, M.; Leiendecker, M.; Das, A.; Poisson, T.; Bui, L. *Chem. Commun.* **2011**, *47*, 10629−10631. (d) Doni, E.; Zhou, S.; Murphy, J. A. *Molecules* **2015**, *20*, 1755−1774.

(11) For other reaction types, see: (a) Zhang, H.; Shi, R.; Ding, A.; Lu, L.; Chen, B.; Lei, A. *Angew. Chem., Int. Ed.* **2012**, *51*, 12542−12545. (b) Drapeau, M. P.; Fabre, I.; Grimaud, L.; Ciofini, I.; Ollevier, T.; Taillefer, M. *Angew. Chem., Int. Ed.* **2015**, *54*, 10587−10591.

(12) (a) Studer, A.; Curran, D. P. *Angew. Chem., Int. Ed.* **2011**, *50*, 5018−5022. (b) Studer, A.; Curran, D. P. *Nat. Chem.* **2014**, *6*, 765−773. (c) Zhou, S.; Anderson, G. M.; Mondal, B.; Doni, E.; Ironmonger, V.; Kranz, M.; Tuttle, T.; Murphy, J. A. *Chem. Sci.* **2014**, *5*, 476−482. (d) Murphy, J. A. *J. Org. Chem.* **2014**, *79*, 3731−3746. (e) Zhou, S.; Doni, E.; Anderson, G. M.; Kane, R. G.; MacDougall, S. W.; Ironmonger, V. M.; Tuttle, T.; Murphy, J. A. *J. Am. Chem. Soc.* **2014**, *136*, 17818−17826. (f) Yi, H.; Jutand, A.; Lei, A. *Chem. Commun.* **2015**, *51*, 545−548. (g) Patil, M. *J. Org. Chem.* **2016**, *81*, 632−639. (h) Barham, J. P.; Coulthard, G.; Kane, R. G.; Delgado, N.; John, M. P.; Murphy, J. A. *Angew. Chem., Int. Ed.* **2016**, *55*, 4492−4496.

(13) DMEDA has also been employed in transition-metal catalyzed C−H arylation reactions as a ligand, see: (a) Liu, W.; Cao, H.; Xin, J.; Jin, L.; Lei, A. *Chem. - Eur. J.* **2011**, *17*, 3588−3592. (b) Liu, W.; Cao, H.; Lei, A. *Angew. Chem., Int. Ed.* **2010**, *49*, 2004−2008.

(14) (a) Connors, K. A. *Chemical Kinetics: The Study of Reaction Rates in Solution*; Wiley-VCH: New York, 1990. (b) Blackmond, D. G. *Angew. Chem., Int. Ed.* **2005**, *44*, 4302−4320. (c) Mathew, J. S.; Klussmann, M.; Iwamura, H.; Valera, F.; Futran, A.; Emanuelsson, E. A. C.; Blackmond, D. G. *J. Org. Chem.* **2006**, *71*, 4711−4722.

(15) In some studies, the reaction progress was monitored (see refs 7a and 7b); however, kinetic order study and kinetic analysis have not been done.

(16) In the framework of *initiation mechanism 3*, a possible pathway for the generation of **3** in the cross-coupling reaction is HAT between 4-methoxyphenyl radical and benzene (see ref 12e). This pathway produces phenyl radical, which then undergoes the coupling reaction with benzene to produce biphenyl in an equal amount to **3**. In the model reaction, this is not the predominant pathway, because only 1.9% of biphenyl was observed as byproduct.

(17) In a control experiment conducted at 80 °C in the absence of DMEDA, small amounts of the coupling product **2** (1.0%) and the byproduct **3** (0.6%) could also be detected. See the Supporting Information for details.

(18) Gans-Eichler, T.; Gudat, D.; Nieger, M. *Angew. Chem., Int. Ed.* **2002**, *41*, 1888−1891.

(19) (a) Dhineshkumar, J.; Lamani, M.; Alagiri, K.; Prabhu, K. R. *Org. Lett.* **2013**, *15*, 1092−1095. (b) Yan, Y.; Xu, Y.; Niu, B.; Xie, H.; Liu, Y. *J. Org. Chem.* **2015**, *80*, 5581−5587.

(20) DFT calculation was performed using the Gaussian 09 software. For full citation of Gaussian 09, see the Supporting Information.

(21) (a) Zhao, Y.; Truhlar, D. G. *Theor. Chem. Acc.* **2008**, *120*, 215−241. (b) Zhao, Y.; Truhlar, D. G. *Acc. Chem. Res.* **2008**, *41*, 157−167.

(22) The calculated potential energy surface for the main chain reaction is shown in the Supporting Information.

(23) Park, J.; Lin, M. C. *J. Phys. Chem. A* **1997**, *101*, 14−18.

(24) The detailed derivation of the rate laws is given in the Support Information.

DOI: 10.1021/jacs.6b03442
J. Am. Chem. Soc. 2016, 138, 7151−7160